Hindawi Publishing Corporation
International Journal of Electrochemistry
Volume 2013, Article ID 138419, 7 pages
http://dx.doi.org/10.1155/2013/138419

Research Article

Simple Formation of Nanostructured Molybdenum Disulfide Thin Films by Electrodeposition

S. K. Ghosh,[1] C. Srivastava,[1] S. Nath,[2] and J. P. Celis[3]

[1] *Materials Processing Division, Bhabha Atomic Research Centre, Trombay, Mumbai 400 085, India*
[2] *Radiation and Photochemistry Division, Bhabha Atomic Research Centre, Trombay, Mumbai 400 085, India*
[3] *Department of Metallurgy and Materials, Katholic University of Leuven, 3001 Leuven, Belgium*

Correspondence should be addressed to S. K. Ghosh; sghosh@barc.gov.in

Received 30 April 2013; Accepted 18 July 2013

Academic Editor: Emmanuel Maisonhaute

Nanostructured molybdenum disulfide thin films were deposited on various substrates by direct current (DC) electrolysis form aqueous electrolyte containing molybdate and sulfide ions. Post deposition annealing at higher temperatures in the range 450–700°C transformed the as-deposited amorphous films to nanocrystalline structure. High temperature X-ray diffraction studies clearly recorded the crystal structure transformations associated with grain growth with increase in annealing temperature. Surface morphology investigations revealed featureless structure in case of as-deposited surface; upon annealing it converts into a surface with protruding nanotubes, nanorods, or dumbbell shape nanofeatures. UV-visible and FTIR spectra confirmed about the presence of Mo-S bonding in the deposited films. Transmission electron microscopic examination showed that the annealed MoS_2 films consist of nanoballs, nanoribbons, and multiple wall nanotubes.

1. Introduction

Molybdenum disulfide, MoS_2, that naturally occurs as molybdenite has layered hexagonal packed structure consisting of –S–Mo–S– sheets stacked one after another by van der Waals interactions. Because of its layered structure, it has got very good lubrication properties due to shearing of layers under the application of normal load. It is perhaps most well-known heterogeneous catalyst in industry for hydrodesulfurization (HDS) of petroleum [1]. Apart from these, due to suitable electron band-gap (~1.7 ev), there is an upsurge interest on MoS_2 solar cell [2] and solar hydrogen production materials [3–5]. Recently DFT calculations [6] showed that in its nanoparticulate form, MoS_2 has demonstrated as promising and inexpensive alternative to platinum for electrochemical and photochemical production of hydrogen from water [7, 8]. It emphasized that presence of edges of S–Mo–S sheet is the active sites; in particular the $[\bar{1}010]$ Mo-edges have the least energy requirement for bonding hydrogen [7–10]. However, precise molecular structure and modes of action of these sites remain unresolved. Therefore, the synthesis of MoS_2 nanoparticulate or nanostructured form having maximum edges of S–Mo–S sheets is of recent investigations concern. Several synthetic approaches like wet inorganic solvent route, template-based, and chemical vapor deposition techniques have been followed [9–15] to prepare such nanoparticulate or nanostructured MoS_2 in order to maximize the sulfide edge effect on hydrogen generation. Synthesis of such MoS_2 nanoparticles or nanostructured forms via stable amorphous precursor followed by crystallization could be a viable alternative. Previous attempts [16–18] for synthesis of MoS_3 or MoS_x films for photovoltaic applications via electrochemical deposition would result in the formation of amorphous films. A heat treatment after film deposition had shown to crystallize the film into *2h*-MoS_2 structure [17]. Therefore, it is important to explore synthesis of MoS_2 films consisting of nanorods, nanotubes, or other nanofeatures via amorphous precursor by electrodeposition.

In the present study, a simple DC electrolysis was employed to produce amorphous MoS_2 film on cathode containing transition metal surfaces. Maintaining very high concentration of sodium sulfide in the electrolyte and using transition metal substrates as cathode material were two major changes adopted in this study in comparison to [16].

In case of former, prevailing idea was to maintain strong H_2S evolution, while electrolysis thereby maximized MoS_2 formation suppressing MoO_x growth. Reason behind using transition metal surface as cathode materials was that, being catalytic in nature, these substrates might accelerate the nanotube/nanorod or nanoball formation during annealing. Therefore, in order to form nanostructured MoS_2 film consisting of several nanofeatures, post deposition films were given suitable annealing treatment. Detailed structural characterization of as-deposited as well as annealed films was carried out utilizing FTIR, UV-visible, X-ray diffraction (XRD), field emission scanning electron microscope (FE-SEM), and transmission electron microscope (TEM).

2. Experimental

DC electrolysis was carried out to deposit MoS_2 films from an electrolyte containing sodium molybdate (0.5 M) and sodium sulfide (30 g/L). The pH of the electrolyte was adjusted to 7 by adding dilute sulphuric acid. A two-electrode system having Pt as anode and substrate as cathode was employed for MoS_2 film growth. Typical substrates used were copper, electroless Ni, and CoW alloy in order to study the catalytic effect of substrates on fullerene/nanotube growth. All these substrates were cleaned first in alkaline solution followed by acid dip in a 10% sulphuric acid solution. Polarization experiments were carried out in EG&G PAR 273 potentiostat/galvanostat. Here, a Pt sheet was used as counter electrode, and Ag/AgCl electrode was used as reference electrode. After deposition, films were annealed in vacuum or in argon atmosphere at 450–600°C for 5 hrs for crystallization. The heating rate was maintained at $5^{\circ}C\,min^{-1}$. A 3D-optical profilometer was used for film thickness determination from step-height measurement. To record Fourier Transform Infrared (FTIR) spectra, Bomem Hartmann and Braun MB Series Infrared spectrometer was used. Annealed MoS_2 (450°C for 5 hrs) powder was crushed with KBr particles (1 : 5) and pressed into thin pellets for FTIR measurements in transmission mode. UV-Vis absorption spectra of annealed MoS_2 powder in water were recorded with JASCO spectrophotometer (model number V-650) using a quartz cell of 1 cm optical path length.

Surface morphology was examined under Philips XL-30 FE-SEM equipped with EDS facility. Both room temperature and high temperature XRD were carried out in Seifert 3003-TT X-ray diffractometer using CuKα1 radiation. For microstructural investigation by TEM, the MoS_2 films were scrapped off from the substrate and dispersed in absolute ethanol (AR grade) by sonication. Then, a drop of this dispersion was placed on carbon coated copper grid and dried in nitrogen before analysis in the TEM (JEOL-2010) operated at 200 kV.

3. Results and Discussions

3.1. Deposition of MoS_2 Films. The electrolytic formation of MoS_2 followed by deposition on the cathode surface is basically a two-step process. First step involves an *in situ* chemical conversion of molybdate to thiomolybdate ions which is followed by electrochemical reduction to MoS_2 at the cathode surface. Addition of initial precursor MoO_4^{2-} and excess of S^{2-} ions gave rise to pH > 12 of the electrolyte. On adding slowly a 10% H_2SO_4 solution, the electrolyte color changed to yellow with release of H_2S gas. Once pH of the electrolyte brought down below 9.0, the electrolyte color became brownish to deep brown. On further addition of acid, the H_2S evolution increased inducing a simultaneous conversion of MoO_4^{2-} to MoS_4^{2-} by the following reaction:

$$MoO_4^{2-} + 6S^{2-} + 12H^+ \longleftrightarrow MoS_4^{2-} + 4H_2O + 2H_2S \uparrow \quad (1)$$

This chemically formed thiomolybdate (MoS_4^{2-}) ion basically acted as precursor for cathodic discharge [16]. This cathodic reduction reaction at the electrode surface results in the *in situ* formation of MoS_x thin films by the following reaction:

$$MoS_4^{2-} + 6H^+ + 2e^- \longleftrightarrow MoS_2 + 2H_2S \uparrow + H_2 \uparrow \quad (2)$$

We note here that the unreacted molybdate (MoO_4^{2-}) ions are also in competition with MoS_4^{2-} ion for discharge at the cathode surface. Therefore, it is required to investigate the polarization curves of sodium molybdate and mixed electrolyte (molybdate-sulfide) individually for selection of voltage/current in order to maximize MoS_2 formation at the cathode surface.

Figure 1 shows the polarization curves of sodium molybdate, sodium sulfide, and molybdate-sulfide mixed electrolyte at pH 7 separately to understand the electrochemical behaviour. We note that the *I-V* curve of sodium sulfide does not have any specific feature except hydrogen evolution. Unlike sodium sulfide, both molybdate and mixed electrolyte ($Na_2MoO_4 + Na_2S$) possess plateau region which is an indication of mixed mode (activation as well-diffusion control) control of discharge of respective species at the cathode surface. Both molybdate and thiomolybdate ions start discharge at ~ −0.283 V versus Ag/AgCl. However, it is seen that at any point of potential, the current density due to discharge of thiomolybdate ion is higher than molybdate ion. On further increase of the potential towards cathodic direction, the current density due to the discharge of thiomolybdate ions exceeds the current density produced by molybdate ions reduction. Therefore, a current density range $\geq 10\,mA{\cdot}cm^{-2}$ was chosen to minimize MoO_2 content in MoS_2 film. Of course, the presence of excess S^{2-} ion in the electrolyte would push the reaction in the forward direction of equation 1 resulting into higher concentration of MoS_4^{2-} ion. Here, thin film deposition were carried out at pH 7.0 so that the electrolyte was kept stable without any precipitation of MoS_3 as would occur at further lower pH. The deposited films were black in color. EDS analysis confirmed composition of the film with S : Mo ~1.7. Figure 2(a) shows 3D surface topography of step edge of MoS_2 films on NiP substrate deposited for a duration of 3 minutes and Figure 2(b) is corresponding 2D pattern. Typical thickness obtained after 3- and 4-minute deposition time was ~400 nm and ~500 nm, respectively, as given in Table 1, and 30–50% film shrinkage

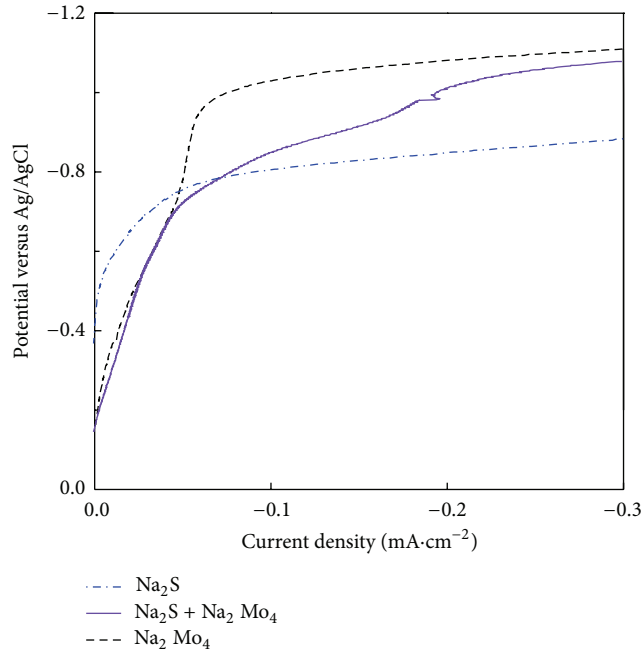

FIGURE 1: Polarization curves of Na_2MoO_4, Na_2S, and Na_2MoO_4 + Na_2S mixed electrolytes. Inset shows enlarged view of onset of discharge potentials for individual electrolytes. Scan rate was 5 mV·s^{-1}.

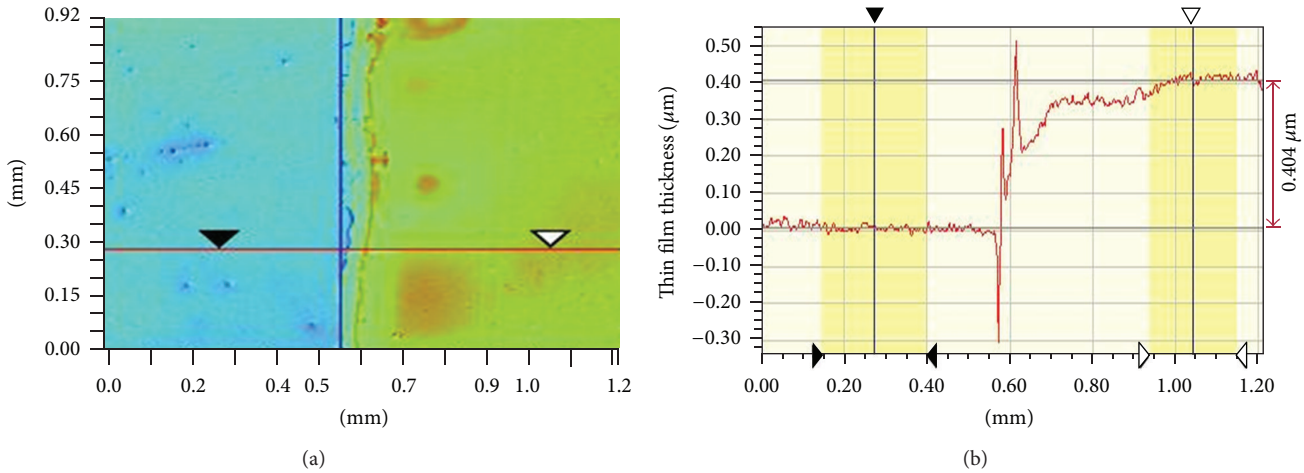

FIGURE 2: (a) 3D surface topography of step edge of MoS_2 films on NiP substrate deposited for a duration of 3 minutes, (b) 2D pattern of line scan of Figure 2(a).

was noticed upon annealing. MoS_2 films were found to peel off from the substrate beyond thickness of 500 nm due to poor adhesion. Film thickness reduction upon annealing could be due to loss of adsorbed water molecules followed by compaction owing to sintering and crystallization process.

The UV-Vis absorption spectrum was measured on scraped annealed (500°C for 5 hrs) MoS_2 powder sample (Figure 3(a)) and shows the features that can be assigned to the A, B, and C excitons, characteristics of the 2H-polytype [19]. The latter two excitons B (625 nm) and C (682 nm) with a splitting of approximately 60 nm corresponds to interlayer interaction and spin-orbit splitting [20]. This is in good agreement with the literature [21]. Normally, a red shift in these two peak positions occurs in case of coaxial MoS_2 nanotubes; however, here the annealed sample seems a mixture of exfoliated MoS_2 with the appearance of shoulder A at 400 nm [20] with other nano-features as can be seen below

TABLE 1: Dependence of MoS_2 thin film thickness on deposition time and heat treatment.

Deposition time (min.)	As-deposited film thickness (nm)	Annealed film thickness (nm)
3	404	223
4	511	341

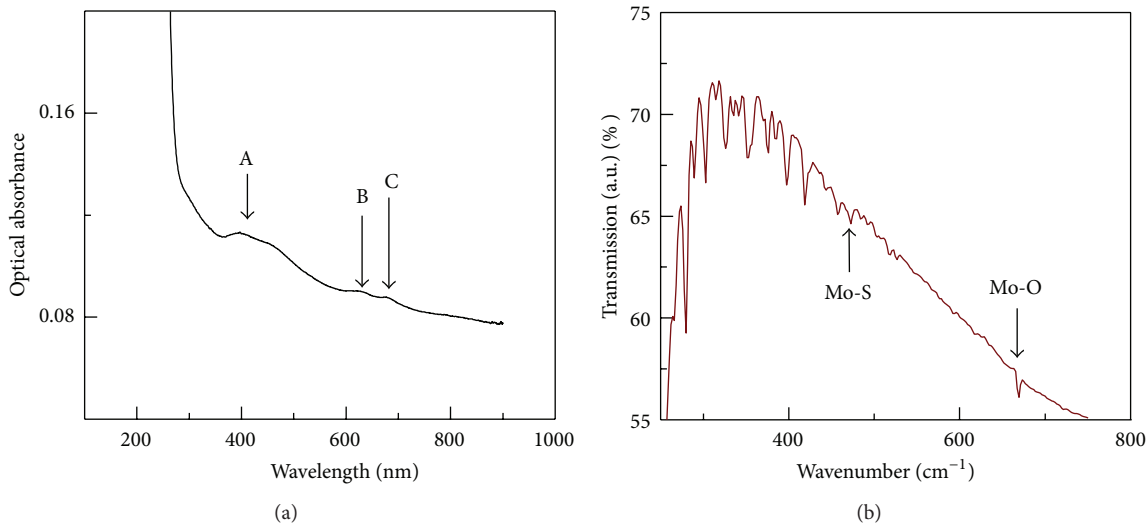

FIGURE 3: (a) UV-visible spectrum of annealed MoS_2 film powder. (b) FTIR spectrum of annealed MoS_2 films. Annealing condition: 450°C for 5 hrs in vacuum.

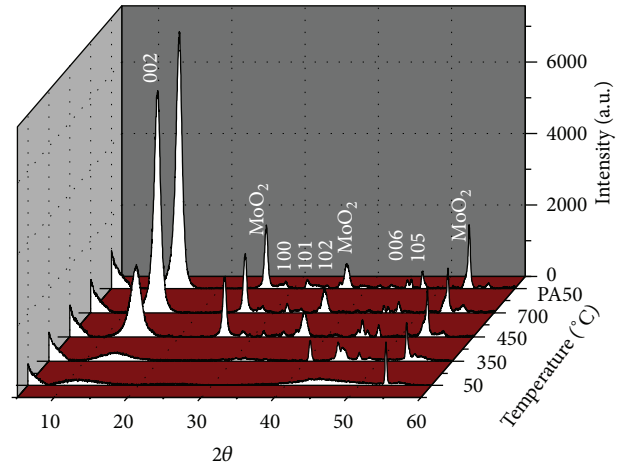

FIGURE 4: XRD pattern of MoS_2 thin film at different temperatures recorded during stepwise annealing. Here "PA50" represents XRD pattern of annealed (700°C) MoS_2 film at 50°C.

from SEM and TEM results. The presence of Mo–S bond in the annealed sample was further ascertained from FTIR spectra as shown in Figure 3(b). The weak peak at 472 cm^{-1} corresponds to Mo–S vibration of MoS_2 [22], and the other band at 690 cm^{-1} match with γ(Mo–O) vibrations [23]. This indicates coexistence of sulfides and oxides in the film.

3.2. Crystal Structure and Phase Analysis. Figure 4 shows XRD pattern of as-deposited as well as annealed MoS_2 films deposited on NiP substrate. It confirms amorphous nature of as-deposited film. In order to study the crystallization process, post deposition films were annealed in argon atmosphere with a heating rate of 5°C min^{-1}, and crystal structure was monitored via *in-situ* XRD. At each temperature, films were hold for 20 minutes for equilibration in crystal structure. The obtained XRD peaks were indexed from ICPDF database and previous literature [13, 24–26]. It is clear from Figure 4 that with increase in temperature, the intensity of hexagonal (002) reflection increases and peak width becomes sharper giving rise to an indication of growth of crystallite sizes. Besides this, other low intensity peaks also start appearing at temperatures ≥ 450°C. The sharp appearance of (002) peak is a clear indication of structural transformation from amorphous to crystalline phases and highly texture along ⟨002⟩ direction. Appearance of low intensity MoO_2 peak suggests presence of minute quantity MoO_2 phases. It supports the FTIR spectra about the presence of oxides in the film along with MoS_2. Detailed peak analysis (position and broadening) of (002) reflections of post annealed 50°C sample (represented as PA50), results into d value of 0.621 nm and grain size of 10 nm. This lattice parameter indicates approximately 97% lattice expansion compared to *2 h* hexagonal structure and matches well with reported inorganic fullerene lattice parameter [13, 26].

3.3. Surface Morphology and Microstructural Investigations. FESEM examination of as-deposited MoS_2 films on NiP substrate results in featureless surface as shown in Figure 5(a).

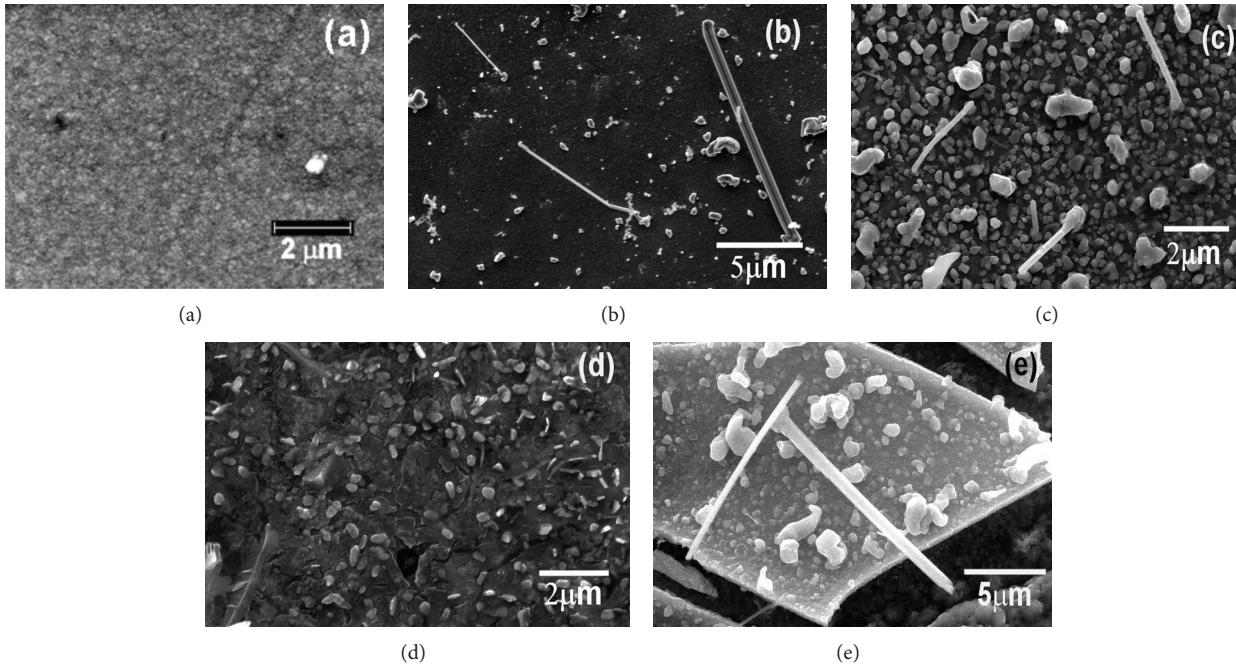

Figure 5: (a) FESEM image of as-deposited MoS_2 films on NiP surface; (b) surface topography of MoS_2 annealed (450°C for 5 hrs) films deposited on NiP substrate showing nanotubes growth; (c) same surface as on (b) showing several nanotube or nanorods growth; (d) Growth of pitta-bread type fullerene structure on CoW surface after annealing at 450°C for 5 hrs, and (e) surface morphology of MoS_2 film on Cu substrate showing film delamination and nanotube/nanorod formation.

Upon annealing at 450°C for 5 hrs, growth of several nanotubes/nanorods, half-cut nanotubes of several micrometer in length with diameter ~10–100 nm, and nanoballs is visible on the surface (Figures 5(b) and 5(c)). We note that the growth of such nanorods/nanotubes is very similar to wishker growth. A close look into the half-cut nanotube (Figure 5(b)) reveals that such nantube surrounds multiple walls of MoS_2 sheets and defect mediated growth. On CoW substrate, MoS_2 fullerenes have grown with different shapes similar to pitta-bread type or hollow dumb-bell shape features (Figure 5(d)) [27]. Figure 5(e) shows surface morphology of annealed MoS_2 film on (450°C for 5 hrs) grown on Cu substrate. Here, the formation of cracks and film delamination associated with growth of nano- and mesotubes/rods and several small protrusions on film layer could be seen. Occurrence of such cracks and film delamination is the result of stress release or due to large difference in thermal expansion coefficient of metal and MoS_2 film.

Figure 6(a) shows transmission electron microscope image of annealed (600°C for 2 hrs) MoS_2 film. TEM investigation of such annealed MoS_2 films revealed that it consisted of several nanofeatures like nanoballs with sizes from 5 to 10 nm and nanosheets or nanoribbons with ~10 nm width and several nanometer in lengths. It seems that formation of nanosheets from the amorphous precursor is the first step. When these nanosheets are sufficient in length, they undergo winding up assuming a hexagonal shape (as shown in Figure 6(a)) to form a nanotube, nanorod, other nanofeatures. It is evident that these sheets are multiple in layers and clear faceting towards the formation of a hexagon. Selected area diffraction (SAED) with spotty ring pattern of annealed MoS_2 film also corroborates the XRD results of well-crystalline nature of the film (inset of Figure 6(a)). Microstructural investigation of annealed MoS_2 film for longer duration (450°C for 5 hrs) reveals the formation of multiwall nanotube as shown in Figure 6(b). It supports the previous section SEM investigation results. Therefore, the microstructure of annealed MoS_2 consists of several nanofeatures starting from nanosheet, nanoribbon, nanoballs, nanoballs, and nanorods/nanoubes depending upon temperature, annealing duration, and substrate.

4. Conclusions

MoS_2 films containing several nano-features like nanoballs, nanorods/nanotubes, and nanoribbons were successfully synthesized by simple DC electrodeposition followed by post annealing treatment. Being a very fast deposition process, a compact MoS_2 film of thickness ~400–500 nm could be obtained within 3-4 minutes duration. X-ray diffraction confirmed the initiation of crystallization process of as-deposited amorphous precursor films at 450°C and higher temperature favors such process. UV-visible and FTIR spectra confirmed the presence of Mo–S as well as Mo–O bonds in the annealed films. FESEM investigations of annealed MoS_2 film (annealed at 450°C for 5 hrs in vacuum or in argon atmosphere) surface revealed the formation of MoS_2 nanoube/nanorod and nanoballs on Ni and Cu substrates and pitta-bread type nanofeatures on CoW substrate. The size of the nanotubes/nanorods varied from 200 nm to 1 micron on Ni and Cu substrates. TEM examinations confirmed the initiation of hexagonal nanotube formation via bending of

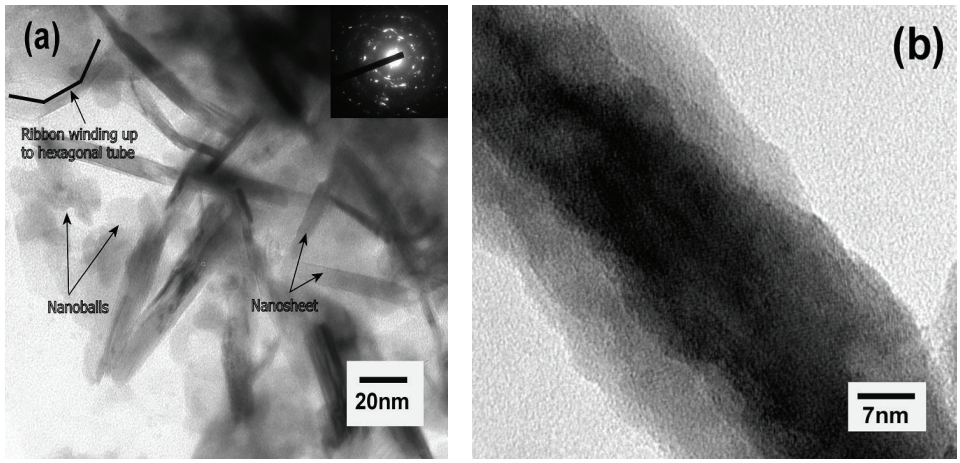

(a) (b)

Figure 6: (a) TEM micrograph showing presence of nanoribbons, nanoballs in postannealed samples (600°C for 2 hrs) and (b) TEM image of multiwall MoS_2 nanotube (450°C for 5 hrs).

nano-ribbons, presence of ribbons, and balls of nanometer in size. It also confirmed the presence of multiple-wall nanotubes. This study unearths that electrodeposition is a simple growth technique for synthesizing nanostructured MoS_2 films which may help in future in making catalyst and/or electrode materials for photoelectrochemical or electrochemical hydrogen production.

Acknowledgments

S. K. Ghosh thanks the European Commission for a Marie Curie Incoming International Fellowship (FP7-PEOPLE-2007-4-2-IIF-220002-NANOCOAT) granted to him under FP-7 framework program. The authors wish to thank Dr. V. Sudarshan, Chemistry Division, Bhabha Atomic Research Centre, for his help in carrying out FTIR spectra.

References

[1] H. Topsøe, B. S. Clausen, and F. E. Massoth, *Hydrotreating Catalysis Science and Technology*, vol. 11, edited by J. R. Anderson and M. Boudart, Springer, New York, NY, USA, 1996.

[2] J. V. Lauritsen, J. Kibsgaard, S. Helveg et al., "Size-dependent structure of MoS_2 nanocrystals," *Nature Nanotechnology*, vol. 2, no. 1, pp. 53–58, 2007.

[3] T. F. Jaramillo, K. P. Jørgensen, J. Bonde, J. H. Nielsen, S. Horch, and I. Chorkendorff, "Identification of active edge sites for electrochemical H_2 evolution from MoS_2 nanocatalysts," *Science*, vol. 317, no. 5834, pp. 100–102, 2007.

[4] T. R. Thurston and J. P. Wilcoxon, "Photooxidation of organic chemicals catalyzed by nanoscale MoS_2," *Journal of Physical Chemistry B*, vol. 103, no. 1, pp. 11–17, 1999.

[5] X. Zong, H. Yan, G. Wu et al., "Enhancement of photocatalytic H_2 evolution on CdS by loading MoS_2 as cocatalyst under visible light irradiation," *Journal of the American Chemical Society*, vol. 130, pp. 7176–7177, 2008.

[6] B. Hinnemann, P. G. Moses, J. Bonde et al., "Biomimetic hydrogen evolution: MoS_2 nanoparticles as catalyst for hydrogen evolution," *Journal of the American Chemical Society*, vol. 127, pp. 5308–5309, 2005.

[7] B. Hinnemann, J. K. Nørskov, and H. Topsøe, "A Density Functional Study of the chemical differences between Type I and Type II MoS_2-based structures in hydrotreating Catalysts," *The Journal of Physical Chemistry B*, vol. 109, no. 6, pp. 2245–2253, 2005.

[8] Y. Li, H. Wang, L. Xie, Y. Liang, G. Hong, and H. Dai, "MoS_2 nanoparticles grown on graphene: an advanced catalyst for the hydrogen evolution reaction," *Journal of the American Chemical Society*, vol. 133, no. 19, pp. 7296–7299, 2011.

[9] H. I. Karunadasa, E. Montalvo, Y. Sun, M. Majda, J. R. Long, and C. J. Chang, "A molecular MoS_2 edge site mimic for catalytic hydrogen generation," *Science*, vol. 335, no. 6069, pp. 698–702, 2012.

[10] A. B. Laursen, S. Kegnaes, S. Dhal, and I. Chorkendroff, "Molybdenum sulfides—efficient and viable materials for electro- and photoelectrocatalytic hydrogen evolution," *Energy & Environmental Science*, vol. 5, pp. 5577–5591, 2012.

[11] L. P. Hansen, Q. M. Ramasse, C. Kisielowski et al., "Atomic—scale edge structures on industrial—style MoS_2 nanocatalysts," *Angewandte Chemie International Edition*, vol. 50, no. 43, pp. 10153–10156, 2011.

[12] J. V. Lauritsen, M. V. Bollinger, E. Lægsgaard et al., "Atomic-scale insight into structure and morphology changes of MoS_2 nanoclusters in hydrotreating catalysts," *Journal of Catalysis*, vol. 221, no. 2, pp. 510–522, 2004.

[13] R. Tenne, Silicon Versus Carbon, NATO Science for Peace and Security Series B: Physics and Biophysics, 2009.

[14] Q. Xiang, J. Yu, and M. Jaroniec, "Synergetic effect of MoS_2 and graphene as cocatalysts for enhanced photocatalytic H_2 production activity of TiO_2 nanoparticles," *Journal of the American Chemical Society*, vol. 134, no. 15, pp. 6575–6578, 2012.

[15] F. Xiangpeng, L. Saifen, S. Yifeng et al., "Lithium storage performance in ordered mesoporous MoS_2 electrode material," *Microporous and Mesoporous Materials*, vol. 151, pp. 418–423, 2012.

[16] E. A. Ponomarev, M. Neumann-Spallart, G. Hodes, and C. Lévy-Clément, "Electrochemical deposition of MoS_2 thin films

by reduction of tetrathiomolybdate," *Thin Solid Films*, vol. 280, no. 1-2, pp. 86–89, 1996.

[17] A. Albu-Yaron, C. Lévy-Clément, A. Katty, S. Bastide, and R. Tenne, "Influence of the electrochemical deposition parameters on the microstructure of MoS_2 thin films," *Thin Solid Films*, vol. 361-362, pp. 223–228, 2000.

[18] R. N. Bhattacharya, C. Y. Lee, F. H. Pollak, and D. M. Schleich, "Optical study of amorphous MoS_3: determination of the fundamental energy gap," *Journal of Non-Crystalline Solids*, vol. 91, no. 2, pp. 235–242, 1987.

[19] R. Coehoorn, C. Haas, J. Dijkstra, and C. J. F. Flipse, "Electronic structure of $MoSe_2$, MoS_2, and WSe_2—I. Band-structure calculations and photoelectron spectroscopy," *Physical Review B*, vol. 35, pp. 6195–6202, 1987.

[20] B. Visic, R. Dominko, M. K. Gunde, N. Hauptman, S. D. Skapin, and M. Remskar, "Optical properties of exfoliated MoS_2 coaxial nanotubes—analogues of graphene," *Nanoscale Research Letters*, vol. 6, article 593, 2011.

[21] G. L. Frey, S. Elani, M. Homyonfer, Y. Feldman, and R. Tenne, "Optical-absorption spectra of inorganic fullerenelike MS_2 (M = Mo, W)," *Physical Review B*, vol. 57, no. 11, pp. 6666–6671, 1998.

[22] S. Liu, X. Zhang, H. Shao, J. Xiu, F. Chen, and Y. Feng, "Preparation of MoS_2 nanofibers by electrospinning," *Materials Letters*, vol. 73, pp. 223–225, 2012.

[23] G. Nagaraju, C. N. Tharamani, G. T. Chandrappa, and J. Livage, "Hydrothermal synthesis of amorphous MoS_2 nanofiber bundles via acidification of ammonium heptamolybdate tetrahydrate," *Nanoscale Research Letters*, vol. 2, no. 9, pp. 461–468, 2007.

[24] M. Chhowalla and G. A. J. Amaratunga, "Thin films of fullerene-like MoS_2 nanoparticles with ultra-low friction and wear," *Nature*, vol. 407, no. 6801, pp. 164–167, 2000.

[25] R. Tenne, L. Margulis, M. Genut, and G. Hodes, "Polyhedral and cylindrical structures of tungsten disulphide," *Nature*, vol. 360, no. 6403, pp. 444–446, 1992.

[26] A. M. Panich, A. I. Shames, R. Rosentsveig, and R. Tenne, "A magnetic resonance study of MoS_2 fullerene-like nanoparticles," *Journal of Physics: Condensed Matter*, vol. 21, Article ID 395301, 39 pages, 2009.

[27] R. Rosentsveig, A. Margolin, A. Gorodnev et al., "Synthesis of fullerene-like MoS_2 nanoparticles and their tribological behavior," *Journal of Materials Chemistry*, vol. 19, no. 25, pp. 4368–4374, 2009.